PHYSICAL REVIEW B VOLUME 56, NUMBER 12 15 SEPTEMBER 1997-II

Theoretical analysis of the magnetic circular dichroism in the $2p3d$ and $2p4d$ x-ray emission of Gd

F. M. F. de Groot
Solid State Physics, University of Groningen, Nijenborgh 4, 9747 AG Groningen, The Netherlands

M. Nakazawa and A. Kotani
Institute for Solid State Physics, University of Tokyo, Roppongi, Minato-ku, Tokyo 106, Japan

M. H. Krisch and F. Sette
European Synchrotron Radiation Facility, Boîte Postale 220, F-38043 Grenoble, France
(Received 24 March 1997)

The $2p3d$ and $2p4d$ x-ray emission spectral shapes have been calculated using a theoretical description of spin-polarized $2p$ photoemission and atomic multiplet calculations of the $2p3d$ and $2p4d$ radiative decay. Emphasis is given to the use of circular-polarized x rays for the excitation process. Good agreement with experiment is found and all visible experimental structures can be explained. It is shown that because of weak multiplet effects in the intermediate state, it is possible to use the incoherent, two-step model. The angle between the emitted x rays and the magnetization is able to affect the magnetic circular dichroism (MCD) spectral shape observed, while the angle between the incident x ray and the magnetization only affects the intensity of the MCD. [S0163-1829(97)01336-2]

I. INTRODUCTION

Due to the presence of more intense synchrotron radiation sources, (resonant) x-ray emission has become an important technique to study the electronic and magnetic structure of solids. A large amount of experimental results have been published in recent years, both on transition metal compounds and rare earths. Experiments on $3d$ transition metal compounds include the $1s3p$ x-ray emission ($K\beta$),[1–4] the $1s2p$ x-ray emission ($K\alpha$) (Ref. 5) and the $2p3d$ resonant x-ray emission.[6–10] In the case of rare earth systems, experiments include the $3d4f$ and $4d4f$ resonant x-ray emission,[11,12] and the $2p3d$ and $2p4d$ resonant x-ray emission.[13–15] A few studies have been carried out with the use of circular polarization.[6,7,15]

The theoretical description of (resonant) x-ray emission is complex and contains many ingredients.[16–20] The main goal of the present paper is to try to describe all these aspects in some detail. With that in mind the paper is written in a rather didactical form, introducing step by step the necessary ingredients. The two important aspects of the theoretical description are (1) the phenomenon of resonant x-ray emission as described by a second order optical process, and (2) the dominance of multiplet effects for core hole states in strongly correlated systems such as transition metals and rare earths. The second order process implies the possibility of strong interference effects, intrinsic angular dependent effects (i.e., independent of the sample symmetry), and the process known as resonant Raman scattering, the scattering via virtual excitations. The consequences of multiplet effects are a complex spectral shape plus a complex resonance/interference behavior.

In the present paper we will concentrate on the theoretical description of the $2p3d$ and $2p4d$ x-ray emission spectra of Gd metal at excitation energies above the $2p$ absorption edge, for which our calculations can be directly compared to existing experimental results.[15] The emission process is described by a combination of $2p$-photoemission and the $2p3d$ and $2p4d$ radiative decay, respectively, while additional effects at the $2p$ resonance are not dealt with quantitatively. These results can be compared to existing experimental results. We start in Sec. II by introducing step by step the theoretical concepts within the two-step, or incoherent model. In Sec. III a comparison is made with the experimental data and in the discussion (Sec. IV) we describe the angular dependence of the x-ray emission process. Finally, the possibility of using the integrated intensities is analyzed.

II. THEORY

Gd is described with an atomic model, only including the seven $4f$ electrons in their Hund's rule ground state ^8S. The intensity of the resonant x-ray emission process is given by

$$I_{(\hbar\omega,\hbar\omega')}=\sum_{q'=0,\pm1}\sum_{q=\pm1}F_{q'q}\cdot\delta_{E_f+\hbar\omega'-E_0-\hbar\omega}, \qquad (1)$$

where the sum extends over the incoming (q) and emitted (q') polarizations. $F_{q'q}$ is described with the Kramers-Heisenberg formula:[16]

$$F_{q'q}=\sum_{\phi_f}\left|\sum_{\phi_x}\frac{\langle\phi_f|C^{(1)}_{q'}|\phi_x\rangle\langle\phi_x|C^{(1)}_{q}|\phi_0\rangle}{E_0+\hbar\omega-E_x-i\Gamma_x}\right|^2, \qquad (2)$$

where ϕ_0 is the $4f^7(^8S)$ ground state. The intermediate state ϕ_x is approximated as $2p^54f^7\varepsilon_d$. The final states are reached via $2p3d$ and $2p4d$ dipole transitions, implying final states such as $3d^94f^7\varepsilon_d$, etc. The dipole transition operator is given with the normalized spherical harmonics

$C_q^{(1)}$, in the following abbreviated to C_q. We take the magnetic field direction, along the sample surface and in the plane of the incident x-ray and the surface normal, as the quantization axis. Then the z-polarized x rays are denoted by C_0 and x- and y-polarized x rays by linear combinations of right circular polarized x-rays C_1 and left circular polarized x-rays C_{-1}. The magnetic circular dichroism (MCD) spectrum is defined by $F_{(q=1)}-F_{(q=-1)}$, taking the incident x-ray direction to be parallel to the magnetization of the Gd $4f$ electrons.

If the intermediate states can be approximated as a single state, or as independent states, the Kramers-Heisenberg formula can be much simplified into a two-step formula removing all the complications of interference and giving an intensity which is the product of x-ray absorption and x-ray emission intensities:

$$F_{q'q}^{[2]}=\sum_{\phi_f}|\langle\phi_f|C_{q'}|\phi_x\rangle|^2\cdot|\langle\phi_x|C_q|\phi_0\rangle|^2. \tag{3}$$

Within this two-step model the $2p3d$ x-ray emission spectral shape is given by the $|\langle 3d^9 4f^7|C_q|2p^5 4f^7\rangle|^2$ matrix element. The matrix element of the excitation, involving the promotion of a $2p$ electron into a continuum state, enters only as a constant. In the following, first the important ingredients of the Hamiltonian for the $2p^5 4f^7$, $3d^9 4f^7$, and $4d^9 4f^7$ states are introduced. At the end of Sec. II B the use of the two-step model will be justified and in Sec. II C the spectral shapes of the x-ray emission are described.

A. Spin-orbit coupling and core-valence exchange

The dominating interaction is the core level spin-orbit coupling (ξ), which splits each core level into two states with an energy difference equal to $\frac{3}{2}\xi$ for $2p$ and $\frac{5}{2}\xi$ for $3d$ and $4d$. The binding energies for the $2p$ core states are, respectively, -7243 eV for $2p_{3/2}$ and -7930 eV for $2p_{1/2}$, split by 687 eV. The binding energies for the $3d$ core states is, respectively -1190 eV for $3d_{5/2}$ and -1222 eV for $3d_{3/2}$, split by 32 eV. For the case of a $4d$ core state, the spin-orbit coupling is smaller than the $4d4f$ and $4f4f$ exchange interactions, hence it is not possible to distinguish $4d_{5/2}$ from $4d_{3/2}$ states. The averaged binding energy is approximately -143 eV. In a first approximation the respective x-ray emission spectra are found at the binding energy differences. For example, the $2p_{3/2}3d_{5/2}$ x-ray emission spectrum is found at -6053 eV, etc.

In order to discuss the consequences of the use of circularly polarized x rays we introduce an exchange splitting between the spin of the core state and the valence states. The valence spin is 7/2 and the $2p$ core hole has $S=1/2$. This gives for each $2p^5 4f^7$ state a splitting into $S=4$ and $S=3$ states. The $2p$ photoemission process can be described in a one-electron picture because the $2p$ spin-orbit is much larger than the $2p4f$ exchange. This gives the ^7P and ^9P configurations of the $2p^5 4f^7$ states. Note that this approximation neglects all configurations other than ^8S of the seven $4f$ electrons, as will be justified below.

Within this one electron picture, the MCD signal at the $2p_{3/2}$ absorption edge is equivalent to the spin-polarized signal.[21,22] Note that the MCD signal follows the orbital moments, the MCD being positive if $m_{j(2p)}$ is positive. This is in contrast to the spin-polarized signal which follows the spin moments, being positive for the ^9P states and negative for the ^7P states.[23,24] It is well known[25] that the spin-up and spin-down spectra can be constructed from the high-spin ^9P-symmetry and the low-spin ^7P-symmetry $2p^5 4f^7$ intermediate states. The ^7P-symmetry state relates for 100% to spin-up, while the ^9P-symmetry state relates for 8/9 to spin-down and for 1/9 to spin-up. Thus the spin-up spectrum is constructed from ^7P + 1/9 ^9P and the spin-down spectrum from 8/9 ^9P, keeping the spin-up to spin-down ratio at 1:1. As noted above, exactly the same is true for the MCD signal.

B. The inclusion of atomic multiplet effects

Using the single-particle picture also for the final states, the $3d^9 4f^7$ final state is split into its $3d_{5/2}$ and $3d_{3/2}$ peaks. Both are split by the $3d4f$ core-valence exchange, implying a splitting between spin-up peaks and spin-down peaks. As discussed above, the MCD signal follows the orbital moment and the MCD signal is reversed with respect to the spin-polarized signal for the $3d_{3/2}$ final state. The result is a plus-minus MCD signal for the $3d_{5/2}$ peak and a minus-plus MCD signal for the $3d_{3/2}$ peak.[23–25] This model is able to explain the gross features of $2p3d$ x-ray emission spectra. There are however additional peaks and structures visible in the experiment and moreover the intensities of the MCD spectra do not exactly follow the pattern as predicted from this model.

There are two, closely related, complications. First, the interaction which was called ''core-valence exchange'' has been presented as a simple exchange interaction, only able to split the spin-up states from the spin-down states. In fact, the ''core-valence exchange'' is a result from the two-electron Coulomb interactions, both exchange $\langle 3d4f|1/r|4f3d\rangle$ and direct $\langle 3d4f|1/r|3d4f\rangle$. The radial integrals related to these three interactions are the Slater integrals $G^{1,3,5}$ and $F^{0,2,4}$, which determine the energy positions of the various symmetry-states of the $3d^9 4f^7$ configuration. These integrals, calculated using the Hartree-Fock based Cowan program[26] for a Gd atom, are given in Table I.

Above we did not consider the $4f4f$ interaction explicitly, but assumed that Gd stayed in its Hunds rule ground state. Like the $3d4f$ interaction, the $4f4f$ interaction gives rise to the Slater integrals $F^{0,2,4,6}$. These $4f4f$ terms determine the complete energy scheme of the $4f^7$ configurations. Apart from the fact that they slightly increase upon creating a core hole (cf. Table I), the $4f^7$ energy scheme is not expected to change. An important consequence is that the combination of the $4f4f$ exchange and the $3d4f$ exchange gives rise to $4f$ transitions from the $8S$ ground state symmetry to another symmetry state in the final state. This process creates peaks at higher energies, hence satellites. This is no surprise for readers familiar with the $3d$ and $4d$ x-ray absorption spectra of Gd, which are completely dominated by multiplet effects and do show a large range of peaks.[27]

In contrast to this, the $2p$-photoemission process can be described as $4f^7(^8S)\rightarrow 2p^5 4f^7(^8S)\varepsilon_d$ and from Table I one finds that the $2p4f$ exchange integrals are about 0.2 eV, which should be compared with the large energy stabilization of the ^8S state due to the $4f4f$ exchange of the order of 7 to 15 eV. Because the ^8S state has an energy far below all

TABLE I. Spin-orbit couplings and the Slater integrals of the $4f4f$ exchange and the core-$4f$ exchange interactions, as calculated with a Hartree-Fock based program for all four configurations indicated. All calculations of the spectral shapes have been carried out using a 80% reduction of all Slater integrals.

	$2p^5 4f^7$	$3d^9 4f^7$	$4d^9 4f^7$	$4f^7$
		Spin-orbit coupling		
ξ_c	478.6	12.4	2.2	
ξ_f	0.242	0.242	0.216	0.197
		$4f4f$ exchange		
F^2	15.973	16.086	15.556	14.505
F^4	10.076	10.157	9.816	9.103
F^6	7.265	7.325	7.078	6.550
		Core-$4f$ exchange		
F^2	2.100	10.303	17.056	
F^4		4.843	10.948	
G^1	0.225	7.451	20.107	
G^3	0.145	4.370	12.693	
G^5		3.019	8.995	

other states and the $2p4f$ exchange is relatively small all intensity goes to the $2p^5 4f^7$ state with the $4f$ electrons in their ^8S configuration. The actual calculation of the $2p$-photoemission process confirms that the intensity to states other than ^8S is less than 0.1% of the total. This justifies the assumption to consider only $2p^5 4f^7(^8S)$ intermediate states. Actually this also justifies the use of the two-step model: if only the ^8S symmetry states are included, no interference effects are possible.

C. The $2p3d$ and $2p4d$ x-ray emission spectral shapes

We will now give the results for the $2p3d$ and $2p4d$ x-ray emission spectral shapes using the atomic multiplet model and the parameters as indicated in Table I. Figure 1 shows the $2p3d$ x-ray emission spectral shapes, that is the transition $2p^5 4f^7[^{7,9}P] \rightarrow 3d^9 4f^7$. Figure 1(a) (bottom, left) shows the $2p_{1/2}3d$ x-ray emission and Fig. 1(b) (top, left) its MCD. Likewise, Fig. 1(c) (bottom, right) shows the $2p_{3/2}3d$ x-ray emission and Fig. 1(d) (top, right) its MCD. Figure 2 repeats these four spectra for the $2p4d$ x-ray emission spectral shapes. A Lorentzian broadening of 2.5 eV [half width at half maximum (HWHM)] of and a Gaussian broadening of 0.75 eV (HWHM) have been used for the broadened spectra. The Lorentzian broadening is given both by the lifetime broadening of the $2p$ hole (about 2.0 eV) and the lifetime broadening of the $3d$ hole (approximated to 0.5 eV). The Gaussian broadening has been chosen to compare the results directly with experiment. The spectra are given with a negative energy axis, indicating that the energy is released from the system in the x-ray emission process.

The main peak of Fig. 1(c) is the $2p_{3/2}3d_{5/2}$ spectrum. The six equidistant large sticks of this spectrum relate to $3d^9 4^7$ states which contain the $4f$ electrons in their ^8S con-

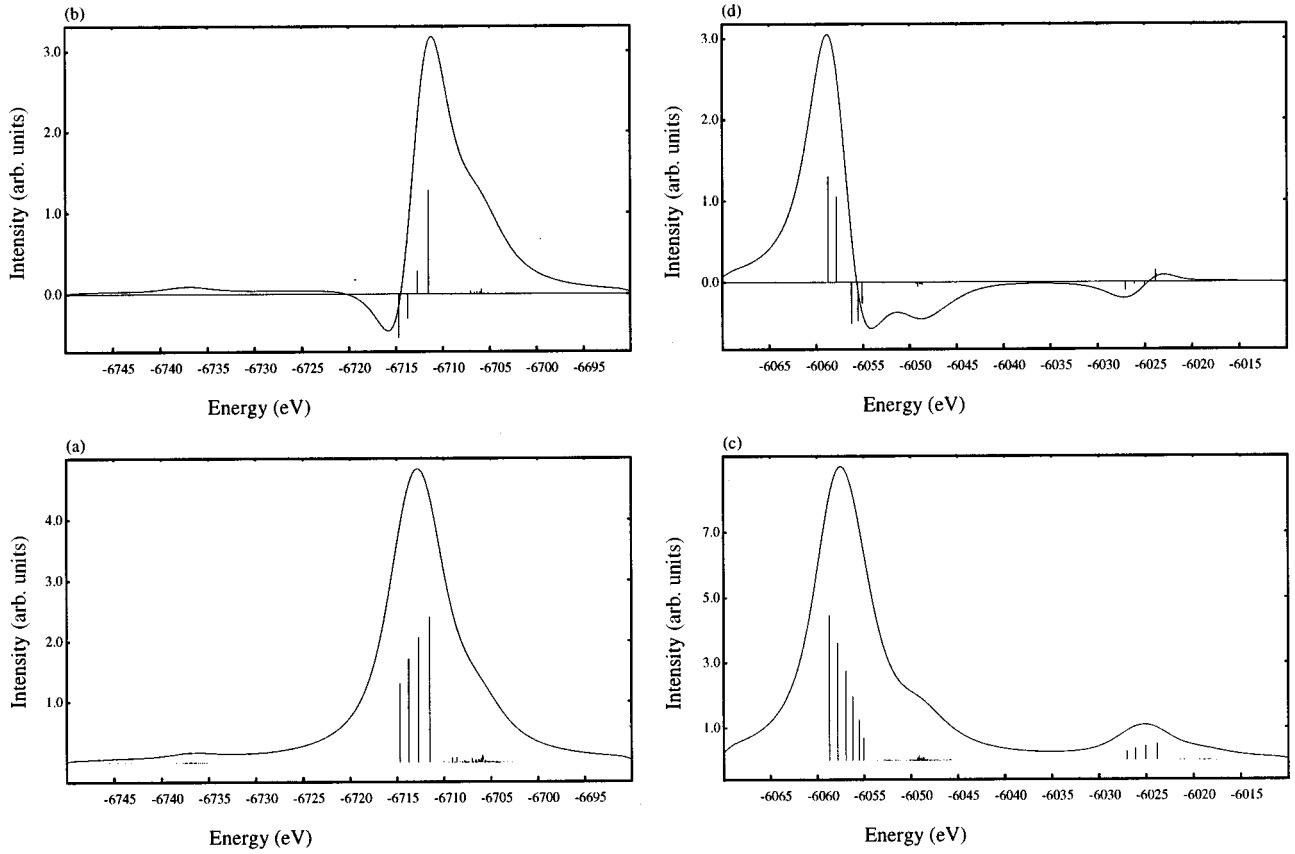

FIG. 1. The $2p3d$ x-ray emission spectral shapes. (a) $2p_{1/2}3d$ x-ray emission, (b) $2p_{1/2}3d$ MCD, (c) $2p_{3/2}3d$ x-ray emission, (d) $2p_{3/2}3d$ MCD. The sticks represent the theoretical intensities. The solid line results from a broadening by a Lorentzian of 2.5 eV and a Gaussian of 0.75 eV (HWHM).

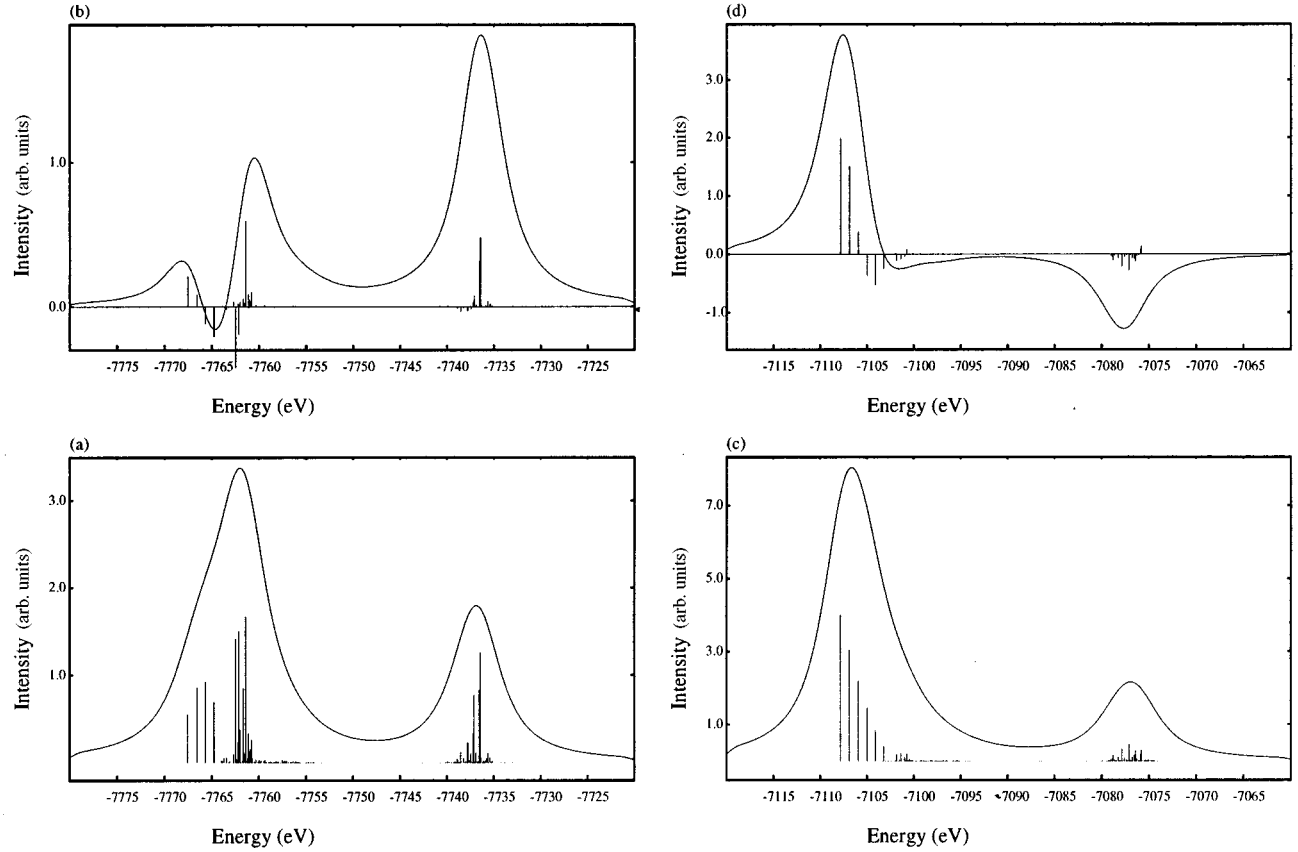

FIG. 2. The $2p4d$ x-ray emission spectral shapes. (a) $2p_{1/2}4d$ x-ray emission, (b) $2p_{1/2}4d$ MCD, (c) $2p_{3/2}4d$ x-ray emission, (d) $2p_{3/2}4d$ MCD. The sticks represent the theoretical intensities. The solid line results from a broadening by a Lorentzian of 2.5 eV and a Gaussian of 0.75 eV (HWHM).

figuration. In that case the $3d^9 4f^7$ symmetries are ^7D and ^9D. The six sticks relate, respectively, to the final states with J_f equal to, respectively, 6, 5, 4, 3, 2, and 1. The large number of small peaks between -6055 eV and -6045 eV are related to transitions for which the $4f$ electrons are in a state different from their ^8S ground state configuration. The most important of these states have the $4f$ electrons in ^6G symmetry, resulting in an overall ^7D, ^7F, and ^7H symmetry of the $3d^9 4f^7$ multiplet. The MCD signal is positive for $2p^5 4f^7$ intermediate states with $J_x=5$ and $J_x=4$ and negative for $J_x=3$ and $J_x=2$. The dipole selection rule ($\Delta J=\pm 1,0$) implies that J_f equal to 6 and 5 are positive, 4 and 3 mixed, and 2 and 1 negative. All small peaks are also essentially negative because only the ^7D states couple to these states. The, positive, ^9D states do not couple apart from minor effects due to spin-orbit coupling. These trends are reproduced at the $2p_{3/2}3d_{3/2}$ transition at -6025 eV. Only four ^8S-related sticks are visible, because $3d_{3/2}$ only couples with ^8S to $J_f=2,3,4,5$. The MCD is reversed due to reversed energy ordering of the J_f states, visible also in the increasing intensity with J_f. The $2p_{1/2}$ spectra [Figs. 1(a) and 1(b)] are closely related to the $2p_{3/2}$ spectra as the $3d^9 4f^7$ final state energies are identical. There are six ^8S sticks for the $3d_{5/2}$ and four sticks for the $3d_{3/2}$. Note that the $2p_{1/2}3d_{5/2}$ transition is not completely zero. It gains some intensity due to the multiplet effects. In other words, the $3d_{5/2}$ and $3d_{3/2}$ structures are slightly mixed.

The $2p4d$ x-ray emission spectra of Fig. 2 look different, reflecting the large $4d4f$ exchange and the small $4d$ spin-orbit coupling. The $2p_{3/2}4d$ spectrum of Fig. 2(c) shows again the six ^8S-related sticks at about -7110 eV. Because the satellite at -7076 eV is caused by $4d4f$ exchange, it contains no ^9D states. All ^9D states are located in the main peak. Note, that we are close to LS coupling and it is more appropriate to speak about $4d^{\uparrow}$ and $4d^{\downarrow}$ parts for the main peak and the satellite, though the MCD shows that this also is only approximate. The ^7D states are mixed much more and are both part of the main peak and the satellite. The highest sticks of the satellite do relate to ^8S-related states of overall ^7D symmetry. In Fig. 2(d) it can be seen that the satellite contains mostly negative sticks, but at the high energy side some positive sticks are visible. In other words the satellite is not 100% spin polarized.

The $2p_{1/2}4d$ spectrum in Figs. 2(a) and 2(b) has the most complex spectral shape. The result of the multiplet effects is a complex spectral shape with highest intensity for the peak at -7762 eV. The spectrum bears little relation to the single-particle model.

III. COMPARISON WITH EXPERIMENT

We will now compare our results to the experiment which has been carried out on beamline ID16/BL21 at the ESRF.[15] For the moment we concentrate on the spectral shapes only and both the x-ray emission spectral shapes and their MCD

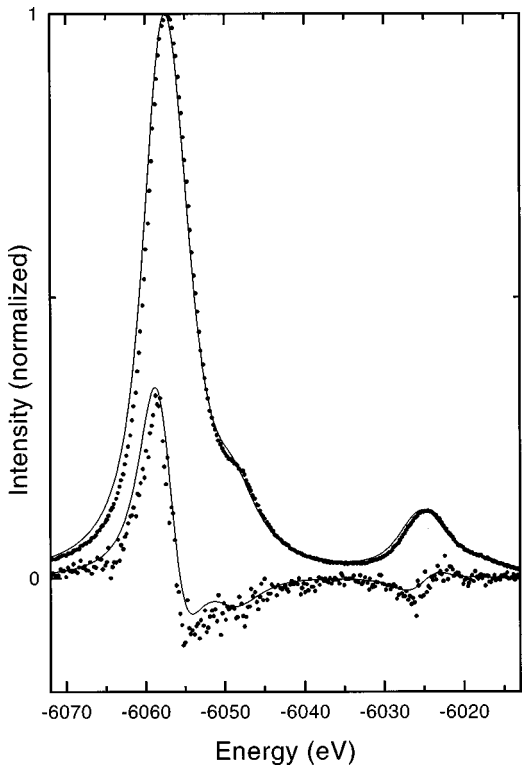

FIG. 3. Comparison of the calculated $2p3d$ x-ray emission spectral shape (solid line), with the $2p_{3/2}3d$ experimental results (points). The experimental curve is aligned and normalized to 1.0 at the peak position, with respect to the calculation. The theoretical MCD spectrum is given in the scale of the emission spectrum, and the experimental MCD has been normalized to it.

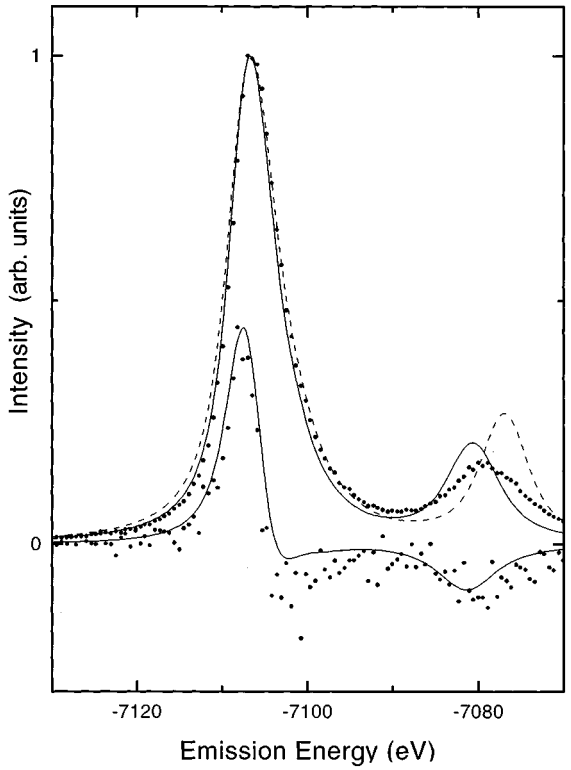

FIG. 4. Comparison of the calculated $2p4d$ x-ray emission spectral shape (dashed), with the $2p_{3/2}4d$ experimental results (points). The experimental curve is aligned and normalized to 1.0 at the peak position, with respect to the calculation. The solid line is the theoretical result with a reduction of the Slater integrals to 70% and a broadening as described in the text. The theoretical MCD spectrum is given in the scale of the emission spectrum, and the experimental MCD has been normalized to it.

will be normalized to the calculations. (In Sec. IV B we will discuss the relative intensities.) The experiments have been performed with an overall resolution of 0.75 eV (HWHM), which will be approximated by a Gaussian in the simulations. The life time broadening of the intermediate and final states is $\Gamma_x = 2.0$ eV and $\Gamma_f = 0.5$ eV, respectively, as determined from the analysis of $2p$ and $3d$ x-ray absorption and photoemission.[28,29] Thus the overall lifetime broadening Γ_T equals 2.5 eV.

Figure 3 shows the comparison of the calculation with the $2p_{3/2}3d$ x-ray emission experiment. The agreement between theory and experiment is good, with the experiment showing slightly sharper structures than the calculations. The relative intensities and peak positions are reproduced, both for the x-ray emission spectral shape as for its MCD. This shows that the approximations made for the simulation are valid. The experiment confirms the reversed MCD effect of the $3d_{3/2}$ peak with respect to the $3d_{5/2}$ peak.

Figure 4 shows the comparison of the calculation with the $2p_{3/2}4d$ x-ray emission experiment. Theoretical results of two x-ray emission and one MCD spectra are shown: The x-ray emission spectrum as plotted in Fig. 2(c), and additionally the x-ray emission and MCD spectra of a second calculation using Slater integrals $G^{1,3,5}$ reduced to 70% (instead of 80%). A similar reduction of the $4d4f$ exchange splitting has been observed also in the analysis of $4d$ x-ray absorption and photoemission spectral shapes.[28] An additional effect of the $4d^9 4f^7$ final state is that its lifetime broadenings are strongly symmetry dependent, and in particular the lifetime broadening of the $4d^{\downarrow}$ structure at -7080 eV is strongly increased to Γ_f of about 1.5 eV (so Γ_T is 3.5 eV), against 0.2 eV ($\Gamma_T = 2.2$ eV) in case of the $4d^{\uparrow}$ structure at -7110 eV.[28,29]

Krisch and co-workers[15] also measured the $2p3d$ x-ray emission spectrum in the vicinity of the $2p_{3/2}$ absorption threshold. If the excitation energy is chosen to be at the $2p \rightarrow 5d$ resonance, the spectral shape can be expected to be affected by the presence of the $5d$ electron and its interaction with the $4f$ electrons. The intermediate state can be described as $2p^5 4f^7 5d^1$ and the $4f5d$ interaction will modify the spectral shape. Preliminary calculations confirm this behavior. At the energy related to the $2p \rightarrow 4f$ transitions, the resonant x-ray emission should reveal an additional feature, arising from the $2p^5 4f^8 \rightarrow 3d^9 4f^8$ transition. Though this feature is clearly visible in the experiment, the spectral shape is dominated by the more intense $3d^9 4f^7 5d^1$ final state multiplet, associated with dipolar $2p \rightarrow 5d$ excitations.

IV. DISCUSSION

A. Angular dependence of x-ray emission

In our calculation made so far, we have assumed that the incident x-ray direction is parallel to the magnetization of the Gd $4f$ electrons and the emitted x-ray is unpolarized. Here we discuss the angular dependence of the x-ray emission MCD. Let us define the angle φ as that between the incident

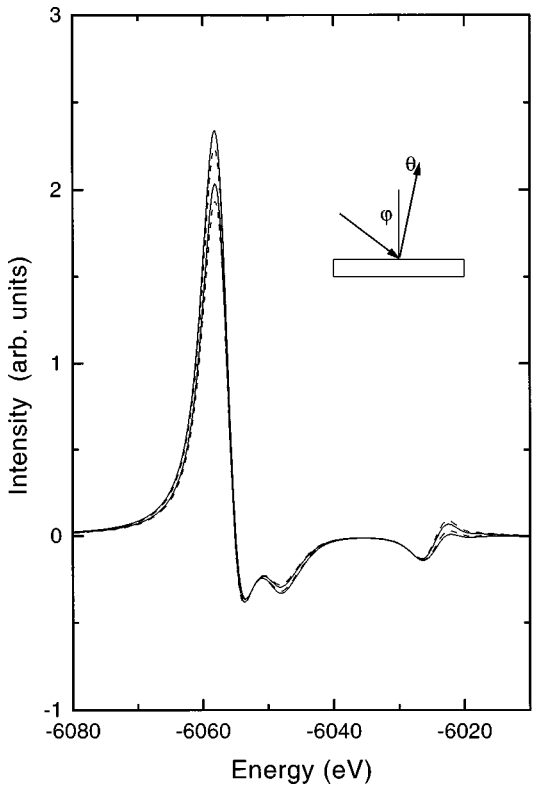

FIG. 5. Angular dependence of the emitted x-ray versus the magnetization direction. Four spectra are given. Viewed at the MCD main peak at -6060 eV, from top to bottom, respectively, the spectra for $\theta=90°$ (solid), 60° (dashed), 30° (solid), and 0° (dashed) are given. The inset shows the definition of the angles ϕ and θ.

x ray and the surface normal, and the angle θ as that between the outgoing x ray and the surface normal (see the inset of Fig. 5). The angular dependence of the MCD intensity is given by

$$\Delta I(\varphi,\theta) = -\frac{1}{2}\sin\varphi[\{1+\sin^2\theta\}(F_{\pm 1-1}-F_{\pm 11}) + 2\cos^2\theta(F_{0-1}-F_{01})], \quad (4)$$

The expression shows that the weight of the spectral intensity $F_{q'q}$ with different polarization depends on the two angles as defined above. First, the factor $\sin\varphi$ originates from the excitation part: $|\langle\phi_x|C_q|\phi_0\rangle|^2$, and the MCD intensity is maximum when the incident x ray is parallel to the magnetization.

The rest of the angular dependent factor of Eq. (1) originates from the deexcitation part: $|\langle\phi_f|C_{q'}|\phi_x\rangle|^2$. If the emission angle θ equals zero, the polarization of the emitted x ray is specified by two directions and ΔI is described by not only the matrix elements of C_1 and C_{-1}, but also C_0. On the other hand, when θ equals 90° ΔI is described by the matrix elements containing only C_1 and C_{-1}.

If we take $1+\sin^2\theta=2\cos^2\theta$, the matrix elements $F_{q'q}$ with different polarization have the same weight. The magic angle between magnetic field and emitted x ray equals $90°-\theta = 54.7°$. In our experimental arrangement, $90°-\theta$ is 60°. Thus the magic angle calculation gives essentially correct results for the experimental situation. The angular dependence of the MCD intensity in $2p3d$ x-ray emission is given in Fig. 5. The main effect is the variation in intensity of the main peak in the $2p_{3/2}3d_{5/2}$ emission region at -6060 eV. The spectrum for magnetization parallel to the sample surface ($\theta=90°$) has the largest MCD. The negative MCD peak at about -6050 eV is not dependent on the emission angle and at higher energies and at the $2p_{3/2}3d_{3/2}$ peak there are some small angular variations visible.

TABLE II. Integrated intensities for the $2p_{3/2}$ and $2p_{1/2}$ x-ray emission spectra, and their MCD divided into their $3d_{5/2}$ and $3d_{3/2}$ parts. The effects of multiplets on the integrated intensities is shown in case of $3d$ and $4d$ final states.

	Intensity		MCD	
$2p_{3/2}$	10		1.111	
$2p_{1/2}$	5		−1.111	
	$3d_{5/2}$	$3d_{3/2}$	$3d_{5/2}$	$3d_{3/2}$
Single particle:				
$2p_{3/2}$	9.000	1.000	1.111	-0.000
$2p_{1/2}$	0.000	5.000	-0.000	-1.111
Multiplet effects:				
$2p_{3/2}$	8.953	1.047	1.188	-0.077
$2p_{1/2}$	0.104	4.896	-0.037	-1.074
	$4d_\uparrow$	$4d_\downarrow$	$4d_\uparrow$	$4d_\downarrow$
Multiplet effects:				
$2p_{3/2}$	8.106	1.892	2.215	-1.105
$2p_{1/2}$	3.515	1.484	-0.372	-0.739

B. The integrated intensities

In the calculation the $2p_{3/2}$ spectra are generated from the addition of the intermediate states $^9P_5$, $^9P_4$, $^7P_3$, and $^7P_2$, normalized to a total intensity of 10. The $2p_{1/2}$ spectra relate to the intermediate states $^7P_4$, $^9P_3$, which add up to 5. This 2:1 ratio is exact as the $2p$ spin-orbit coupling is large. For the $2p_{3/2}3d$ x-ray emission, the ratio of the x-ray emission spectrosocpy (XES) and the MCD integral is 1/9. The reason is that the ^9P states are not pure spin-up, but contain 1/9 spin-down character as discussed above. The consequence is that the integrated MCD signal of the $2p_{3/2}$ spectra is 10/9. This MCD signal is exactly compensated at the $2p_{1/2}$ spectra, as can be checked from Table II, which collects all integrated values. The integrated value I_{MCD} over both edges is zero, as it should be for $2p$ core states containing equal amounts of spin-up and spin-down electrons.

In Table II the integrated quantities for $2p_{3/2}$ and $2p_{1/2}$ have been divided into transitions to, respectively, $3d_{5/2}$ and $3d_{3/2}$. It can be seen that, if the full atomic multiplet interactions are included, the respective integrated intensities for the four $2p3d$ spectra do differ only a few percent from the single-particle values. Therefore one can conclude that the multiplet effects cause a redistribution of intensity within a particular x-ray emission spectrum (with the creation of extra peaks), but the multiplet effects are too small to significantly affect the integrated intensities. The reason is that the $3d$

spin-orbit splitting of 32 eV is larger than all multiplet effects, causing only a small admixture of the $2p_{3/2}3d_{5/2}$ and $2p_{3/2}3d_{3/2}$ spectra.

In the case of the $4d4f$ x-ray emission spectra, the relation with the exchange-plus-spin-orbit model is lost because now the $4d4f$ exchange is larger than the $4d$ spin-orbit coupling. The $4d$ states are in Table II indicated with $4d_{\uparrow}$ implicitly assuming pure LS coupling. The actual situation is that the $4d^9 4f^7$ states are in between the jj and LS coupling schemes. It is important to note that if one excites in between the L_3 and L_2 edge, the integrated $2p3d$ and $2p4d$ x-ray emission intensity will always contain an MCD effect (cf. Table II), which implies that fluorescence-yield detection of x-ray absorption MCD cannot be normalized in between the L_3 and L_2 edges.

Concerning the magnetic moments it is clear that no information can be gained from the absorption sum rules, because the sum rules concern the $2p$ core state which is filled in the ground state, hence all moments are zero. However, information concerning the magnetic moment could be gained from the magnitude of the MCD effect in the emission, where the MCD is normalized to the total intensity as MCD/XES. The magnitude of the MCD in the emission is dependent on a series of factors. It depends on the degree of circular polarization incident on the sample (70%) and cf. Eq. (4) on the angle between the incident x rays and the magnetic field (30°). The as such corrected and normalized MCD reaches approximately 17% in experiment. Because the experimental value for the emission angle (60°) is close to the magic angle (54°), the experimental result is close to the angle-integrated calculation. Comparing the experimental value of 17% with the theoretical maximal value of 33% (cf. Fig. 1), gives an effective magnetization of about 1/2 of the maximum in the experiment.

C. Concluding remarks

Using the theoretical description of spin-polarized $2p$-photoemission and the atomic multiplet calculations of $2p3d$ and $2p4d$ x-ray emission, all $2p3d$ and $2p4d$ x-ray emission spectral shapes have been calculated, including their dependence on the use of circular-polarized x rays for the excitation process. Good agreement with experiment is found and all visible experimental structures have been explained. The present analysis confirms the importance of multiplet effects for the spectral shapes of $3d$ and $4d$ holes in rare earths.

It is shown that the multiplet effects do not alter the integrated values of the $2p3d$ x-ray emission peaks and their MCD, in contrast to the $2p4d$ x-ray emission peaks. Because the x-ray emission spectra relate to an excitation process to a continuum state, the overall integral of the MCD should be equal to zero. However from the size of the MCD spectral shapes compared with the calculations, information on the magnetic moment can be gained.

It is shown that the angle of incidence between x ray and surface normal influences the size of the MCD effect, while the angle of emittance between x-ray and surface normal influences the spectral shape of the MCD.

ACKNOWLEDGMENTS

The research of F.dG. has been made possible by the Royal Netherlands Academy of Arts and Sciences (KNAW). This work is partially supported by a Grant-in-Aid for Scientific Research from the Ministry of Education, Science, Sports and Culture in Japan. The computation in this work was partly done using the facilities of the Supercomputer Center, Institute for Solid State Physics, University of Tokyo.

[1] K. Hämäläinen, C.C. Kao, J.B. Hastings, D.P. Siddons, L.E. Berman, V. Stojanoff, and S.P. Cramer, Phys. Rev. B **46**, 14 274 (1992).

[2] G. Peng, F.M.F. de Groot, K. Hämäläinen, J.A. Moore, X. Wang, M.M. Grush, J.B. Hastings, D.P. Siddons, W.H. Armstrong, O.C. Mullins, and S.P. Cramer, J. Am. Chem. Soc. **116**, 2914 (1994).

[3] F.M.F. de Groot, A. Fontaine, C.C. Kao, and M. Krisch, J. Phys.: Condens. Matter **6**, 6875 (1994).

[4] Throughout the paper we use the notation $1s2p$, instead of the other familiar notation ($K\alpha$, etc).

[5] X. Wang, F.M.F. de Groot, and S.P. Cramer, Phys. Rev. B. (to be published).

[6] C.F. Hague, J.M. Mariot, P. Strange, P.J. Durham, and B.L. Gyorffy, Phys. Rev. B **48**, 3560 (1993).

[7] L.C. Duda, J. Stöhr, D.C. Mancini, A. Nilsson, N. Wassdahl, J. Nordgren, and M.G. Samant, Phys. Rev. B **50**, 16 758 (1994).

[8] S. Shin, A. Agui, M. Watanabe, M. Fujisawa, Y. Tezuka, and T. Ishii, J. Electron Spectrosc. Relat. Phenom. **79**, 125 (1996).

[9] Y. Tezuka, S. Shin, A. Agui, M. Fujisawa, and T. Ishii, J. Phys. Soc. Jpn. **65**, 312 (1996).

[10] S.M. Butorin, J.H. Guo, M. Magnuson, P. Kuiper, and J. Nordgren, Phys. Rev. B **54**, 4405 (1996).

[11] S.M. Butorin, D.C. Mancini, J.H. Guo, N. Wassdahl, J. Nordgren, M. Nakazawa, S. Tanaka, T. Uozumi, A. Kotani, Y. Ma, K.E. Myano, B.A. Karlin, and D.K. Shuh Phys. Rev. Lett. **77**, 574 (1996).

[12] J.J. Gallet, J.M. Mariot, C.F. Hague, F. Sirotti, M. Nakazawa, H. Ogasawara, and A. Kotani, Phys. Rev. B **54**, 14 238 (1996).

[13] K. Hämäläinen, D.P. Siddons, J.B. Hastings, and L.E. Berman, Phys. Rev. Lett. **67**, 2850 (1991).

[14] M. Krisch, C.C. Kao, F. Sette, W.A. Caliebe, K. Hämäläinen, and J.B. Hastings, Phys. Rev. Lett. **74**, 4931 (1995).

[15] M. Krisch, F. Sette, U. Bergmann, C. Masciovecchio, R. Verbeni, J. Goulon, W. Caliebe, and C.C. Kao, Phys. Rev. B **54**, 12 673 (1996).

[16] J. Tulkki and T. Åberg, J. Phys. B **13**, 3341 (1980); **15**, L435 (1982); T. Åberg and B. Crasemann, in *X-ray Anomalous (Resonance) Scattering: Theory and Experiment*, edited by K. Fisher, G. Materlik, and C. Sparks (Elsevier, Amsterdam, 1994).

[17] P. Carra, M. Fabrizio, and B.T. Thole, Phys. Rev. Lett. **74**, 3700 (1995).

[18] A. Kotani, J. Phys. (Paris) Colloq. **7**, C2-1 (1997).

[19] M. Nakazawa, S. Tanaka, T. Uozumi, and A. Kotani, J. Phys. Soc. Jpn. **65**, 2303 (1996).

[20] F.M.F. de Groot, Phys. Rev. B **53**, 7099 (1996).

[21] N.V. Smith, C.T. Chen, F. Sette, and L.F. Mattheiss, Phys. Rev. B **46**, 1023 (1992).
[22] F.M.F. de Groot, in *X-ray and Inner Shell Processes*, edited by R. L. Johnson, H. Schmidt-Böcking, and B. F. Sonntag, AIP Conf. Proc. No. 389 (AIP, Woodbury, NY, 1997), p. 497.
[23] G. van der Laan, Phys. Rev. B **51**, 240 (1995).
[24] G. van der Laan and B.T. Thole, Phys. Rev. B **48**, 210 (1993).
[25] T. Kachel, C. Carbone, and W. Gudat, Phys. Rev. B **47**, 15 391 (1993).
[26] R.D. Cowan, *The Theory of Atomic Structure and Spectra* (University of California Press, Berkeley, 1981).
[27] J.B. Goedkoop, B.T. Thole, G. van der Laan, G.A. Sawatzky, F.M.F. de Groot, and J.C. Fuggle, Phys. Rev. B **37**, 2086 (1988).
[28] H. Ogasawara, A. Kotani, and B.T. Thole, Phys. Rev. B **50**, 12 332 (1994).
[29] K. Okada, A. Kotani, H. Ogasawara, Y. Seino, and B.T. Thole, Phys. Rev. B **47**, 6203 (1993).